Title

Tracking Aqueous Proton Transfer by Two-Dimensional Infrared Spectroscopy and ab Initio Molecular Dynamics Simulations

Journal

ACS Central Science, 5(7)

ISSN

2374-7943

Authors

Yuan, Rongfeng
Napoli, Joseph A
Yan, Chang
et al.

Publication Date

2019-07-24

DOI

10.1021/acscentsci.9b00447

Peer reviewed

ACS central science

Research Article

Cite This: ACS Cent. Sci. 2019, 5, 1269–1277

http://pubs.acs.org/journal/acscii

Tracking Aqueous Proton Transfer by Two-Dimensional Infrared Spectroscopy and ab Initio Molecular Dynamics Simulations

Rongfeng Yuan,[†,#] Joseph A. Napoli,[†,#] Chang Yan,[†,§] Ondrej Marsalek,[‡] Thomas E. Markland,*[,†] and Michael D. Fayer*[,†]

[†]Department of Chemistry, Stanford University, Stanford, California 94305, United States

[‡]Charles University, Faculty of Mathematics and Physics, Ke Karlovu 3, 121 16 Prague 2, Czech Republic

Supporting Information

ABSTRACT: Proton transfer in water is ubiquitous and a critical elementary event that, via proton hopping between water molecules, enables protons to diffuse much faster than other ions. The problem of the anomalous nature of proton transport in water was first identified by Grotthuss over 200 years ago. In spite of a vast amount of modern research effort, there are still many unanswered questions about proton transport in water. An experimental determination of the proton hopping time has remained elusive due to its ultrafast nature and the lack of direct experimental observables. Here, we use two-dimensional infrared spectroscopy to extract the chemical exchange rates between hydronium and water in acid solutions using a vibrational probe, methyl thiocyanate.

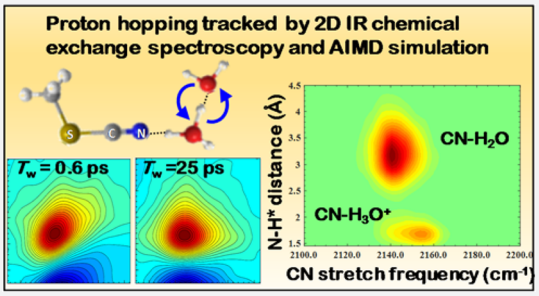

Ab initio molecular dynamics (AIMD) simulations demonstrate that the chemical exchange is dominated by proton hopping. The observed experimental and simulated acid concentration dependence then allow us to extrapolate the measured single step proton hopping time to the dilute limit, which, within error, gives the same value as inferred from measurements of the proton mobility and NMR line width analysis. In addition to obtaining the proton hopping time in the dilute limit from direct measurements and AIMD simulations, the results indicate that proton hopping in dilute acid solutions is induced by the concerted multi-water molecule hydrogen bond rearrangement that occurs in pure water. This proposition on the dynamics that drive proton hopping is confirmed by a combination of experimental results from the literature.

I. INTRODUCTION

Proton transport in water is a central step in many natural and technological processes. In aqueous systems, protons can diffuse much more rapidly than water molecules or small cations owing to proton relay in the structural diffusion mechanism, as opposed to a vehicular mechanism for other metal cations.[1] Structural diffusion describes proton diffusion as occurring via hops between water molecules.[1] The anomalously rapid diffusion of protons in water was first noted by Grotthuss in an 1806 paper,[2] and hence the mechanism is frequently referred to as the Grotthuss mechanism, although he did not present the molecular-level picture. The atomistic details of this mechanism have been the focus of extensive experimental and theoretical work to elucidate the structures the proton forms in solution, the mechanisms for their interconversion, and how to probe them spectroscopically.[3−22] In a simplified physical picture, the fundamental event is proton transfer from a hydronium cation (H_3O^+), which is a water molecule with an extra proton (proton defect), to one of the water molecules to which it is hydrogen bonded. The newly formed H_3O^+ then transfers a proton, which is not necessarily the same proton, to another water molecule. This process is referred to as proton hopping. For over 200 years, there has been no direct observation of the time it takes a proton to move from a hydronium cation to the water molecule which receives the proton. Experimental determination of this proton transfer time has proven to be a major challenge. Here, we overcome this challenge by experimentally obtaining the proton hopping times in concentrated hydrochloric (HCl) acid solutions and demonstrate that this hopping time can be extrapolated to the dilute limit. Within error, the dilute limit hopping time obtained here is the same as that inferred from measurement of the proton diffusion constant.[6,23,24] In addition, the proton hopping time is the same as the time for concerted hydrogen bond (H-bond) rearrangement in pure water, suggesting that it is the water H-bond rearrangement that induces proton hopping.

In solution, the proton defect is solvated by water molecules which form H-bonds that stabilize it in its local environment. Within a given solvation environment, transient local deformations such as proton rattling and bending and stretching of the hydronium occur on a time scale of ∼100 fs.[7,9,16,25] Over longer picosecond time scales, structural reorganization of the H-bond network occurs,[6,19,26] which alters the solvation environment of the proton defect and allows proton transfer to neighboring water molecules to occur when they can better stabilize the proton. The longer time

Received: May 5, 2019
Published: May 23, 2019

DOI: 10.1021/acscentsci.9b00447
ACS Cent. Sci. 2019, 5, 1269−1277

scale has previously been determined using static NMR measurements with line width analysis[6] and ionic mobility experiments based on a Gaussian diffusion model,[26] both of which are heavily model dependent. Hence, direct time-resolved measurements of the proton transfer dynamics are important and useful to elucidate details of the proton hopping process.

H-bond dynamics of pure water[27] as well as water−ion complex dynamics[28] have been successfully addressed using ultrafast nonlinear infrared experiments performed on the OD or OH hydroxyl stretch of HOD vibrational probes in H_2O or D_2O. However, to perform experiments on the hydronium ion requires a hydronium concentration that approaches that of water; i.e., the experiments require using highly concentrated acid solutions. In such solutions, time-dependent infrared measurements of the proton transfer rate have not been possible due to the extremely broad and heavily overlapping IR absorption spectra of the water and hydronium species[5,15] and the short vibrational lifetimes of the OH or OD vibrational probes, usually of less than 1 ps in acidic solution.[7,16] As such, recent experiments were only able to place a lower bound of 480 fs on the time scale[17] and suggest an upper limit of ∼2.5 ps.[16]

Here, a new approach was successfully applied. Two-dimensional infrared (2D IR) chemical exchange experiments were performed on a long-lived vibrational probe with a well-defined absorption line shape. The chemical exchange experiments yielded the time for a hydronium ion to transfer a proton and become a water molecule and for a water molecule to receive a proton and become a hydronium. Ab initio molecular dynamics (AIMD) simulations provided molecular-level understanding of the observables and are the key to understanding and determining the proton hopping time. Experimental and simulation concentration studies permitted the measured transfer times to be extrapolated to infinite acid dilution. The results presented here are consistent with the previous indirect determinations of the single step proton hopping time,[6,26] and utilization of experimental results from the literature[23,29,30] leads to the conclusion that proton hopping is driven by the concerted hydrogen bond (H-bond) rearrangement that occurs in pure water.

II. RESULTS AND DISCUSSION

A. Experiments. Water and hydronium are in equilibrium in concentrated HCl solutions. Hence when looking at a particular oxygen atom, sometimes it forms part of a water molecule and sometimes it forms part of a hydronium cation, which interconvert as protons move on and off the oxygen. The key questions are how long does it take for a proton to move off the oxygen (hydronium to water), and how long does it take for a proton to move onto the oxygen atom (water to hydronium)?

2D IR chemical exchange spectroscopy has been applied to a variety of systems.[28,31] For two species, A and B, with different vibrational spectra for a given vibrational mode, at short time (T_w) the 2D spectrum has two peaks on the diagonal. Because the system is in equilibrium, A converts to B and vice versa, with no net change in the A and B concentrations. The interconversion of species causes off-diagonal peaks to grow in as T_w is increased, one peak for A → B and the other for B → A. Detailed analysis of the off-diagonal and diagonal peak volume time dependences, combined with the equilibrium constant, gives the two rate constants.

There are four pulses in a 2D IR experiment. The first pulse labels the molecules with their initial vibrational frequencies, and the second pulse stores this information. The third pulse, after a variable waiting time T_w, stimulates the emission of the echo pulse, which reads out the final frequencies. When T_w is very short, final frequencies are the same as the initial frequencies, so the 2D spectrum has only diagonal peaks. As T_w becomes longer, because of the chemical exchange there are new final frequencies, the off-diagonal peaks. Providing that the peaks in the FT-IR spectrum can be assigned to the species, then chemical exchange data can be extracted from the 2D spectra even if the Fourier transform IR (FT-IR) spectra of the two species overlap extensively.[28] To use 2D IR chemical exchange spectroscopy to measure the water-hydronium chemical exchange, we have employed a new vibrational probe, the CN stretch of methyl thiocyanate (MeSCN). The N lone pair is an H-bond acceptor for both water and hydronium. Figure 1A shows FT-IR spectra of the CN stretch as a function

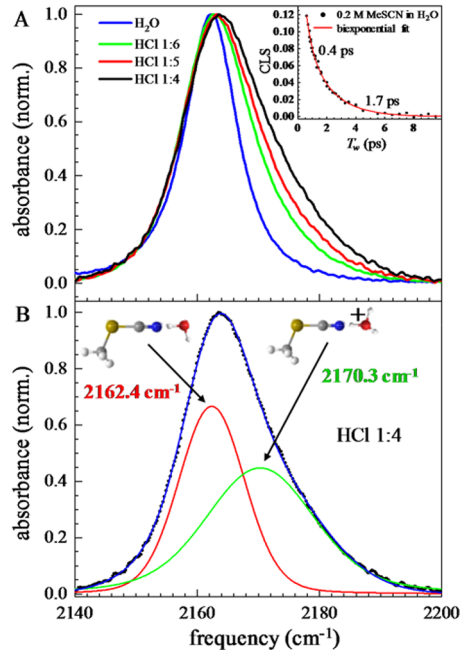

Figure 1. (A) CN stretch spectra of MeSCN in water and in several HCl solutions of high concentration. As the HCl concentration increases, the shoulder on the high-frequency side increases in amplitude. Inset: Spectral diffusion data from the CN stretch in pure water. The decay constants are the same as those reported previously using the water hydroxyl stretch (OD of HOD in H_2O) showing the MeSCN is an accurate reporter of water dynamics. (B) CN stretch spectrum decomposed into bands corresponding to water H-bonded to the N of CN (red curve) and hydronium H-bonded to N (green curve).

of HCl concentration. The blue curve, a narrow symmetric peak centered at 2162 cm^{-1}, is the spectrum in pure H_2O. The inset shows the results of 2D IR spectral diffusion experiments on H_2O using MeSCN. For a single component system, spectral diffusion reports on the dynamics of the system, i.e., water H-bond dynamics.[27] The data were fit with a biexponential, yielding time constants that are identical to those measured using the OD stretch of HOD in H_2O.[32] Simulations show that the 0.4 ps time constant arises from small local H-bond motions, while the 1.7 ps time constant is the H-bond rearrangement time.[27] Therefore, the CN stretch

DOI: 10.1021/acscentsci.9b00447
ACS Cent. Sci. 2019, 5, 1269−1277

of MeSCN accurately reports on the H-bond dynamics in water. This also indicates that MeSCN induces negligible perturbation to the dynamics of the hydrogen bond network, which further validates the application of this probe in concentrated acid solutions.

Recently, the use of MeSCN in lithium chloride (LiCl) solutions in which the CN stretch has two distinct absorption peaks, one corresponding to the nitrogen lone pair H-bonded to water (water-associated state) and the other related to the Li^+-associated MeSCN, was reported. The two distinct peaks in the spectrum arise because of substantial electrostatic interaction.[32] The observations on the LiCl solutions and the concentration dependence shown in Figure 1A demonstrate that the growing absorption shoulder on the high-frequency side as HCl concentration increases corresponds to an emergent hydronium-associated state (H), while the peak position of the original water-associated state (W) remains unchanged within experimental error. Assuming that the two components' absorption line shapes are constant for the three HCl concentrations, scaled subtraction leads to the separation of H and W states. Figure 1B shows the spectrum of 10.8 M HCl (1:4 HCl/water) and the two component fit to the spectrum (see Supporting Information). The red curve, water H-bonded to the nitrogen, is almost identical to the peak in pure water. The green curve, hydronium H-bonded to the nitrogen, is broader and shifted to a higher frequency by 7.9 cm^{-1}. The sum of these two components reproduces the absorption spectra of the other two HCl solutions very well. While the two peaks overlap substantially, the spectral separation is sufficient to perform the chemical exchange experiments.

Figure 2 presents representative chemical exchange data for the 10.8 M HCl solution. The two columns show short time (T_w = 0.6 ps, left) and long time (T_w = 25 ps, right) data and calculations. The top row is experimental data. At 0.6 ps, there has been insufficient time for water and hydronium to interconvert to any significant extent, and there are at most very small indications of the initial growth of off-diagonal peaks. By 25 ps, substantial chemical exchange has occurred, and the off-diagonal exchange peaks are prominent. The data were quantitatively analyzed at many T_w's as described in the Supporting Information and previously.[32] The second row shows modeled data using rate equations and 2D Gaussian functions, which do an excellent job of reproducing the experimental data. Modeled data are used to extract the diagonal and off-diagonal peak volumes at each T_w. The third row contains calculated data but with chemical exchange turned off in the calculations. Comparing the right-hand panel of the third row to the first and second rows clearly demonstrates the influence of chemical exchange on the 2D spectra. The chemical exchange can be modeled with the following equation

$$\mathrm{MeSCN{\cdot}H_3O^+\ (H)} \underset{k_{WH}}{\overset{k_{HW}}{\rightleftharpoons}} \mathrm{MeSCN{\cdot}H_2O\ (W)} \quad (1)$$

where k_{HW} and k_{WH} corresponds to the rates for the interconversion between H and W. With additional consideration of vibrational lifetimes, one can use a general rate scheme (see Supporting Information) to fit the experimental population evolution data. Because the relation between k_{HW} and k_{WH} is fixed by an equilibrium constant, which was measured separately, there are only three adjustable parameters: the exchange rate, the CN stretch lifetime for water-bound CN, and the lifetime for hydronium-bound CN. The lifetimes were obtained by fits to all three concentrations to improve accuracy; i.e., only the exchange rate (k_{HW} or k_{WH}) changes with the HCl concentration.

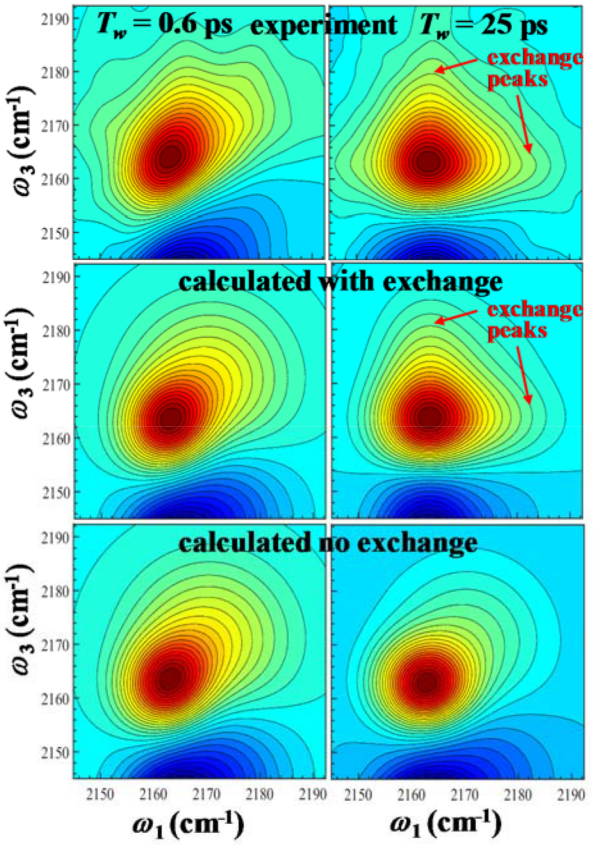

Figure 2. Two-dimensional IR experimental and calculated spectra at two times showing the effects of chemical exchange. Top: The off-diagonal chemical exchange peaks have grown in by T_w = 25 ps. Middle: Spectra calculated using the chemical exchange kinetic equations, which reproduce the data very well. Bottom: Spectra calculated leaving the chemical exchange terms out of the kinetic equations. The off-diagonal peaks are absent.

Figure 3 displays the time dependence of the 2D spectra for the three HCl concentrations (see Figure 1), namely, the molar ratio of HCl to water being 1:4, 1:5, and 1:6. The circles are the data. The solid curves are the simultaneous fits of the parameters in the rate scheme (see Supporting Information) with one set of parameters for all of the data in each panel. The diagonal peaks (black and red data and fits) decay because of the vibrational lifetimes and chemical exchange. The off-diagonal peaks (blue data and fits) increase because of chemical exchange and decay because of the lifetimes. The kinetic model involves the following chemical equilibrium

$$\mathrm{MeSCN{\cdot}H_3O^+ + H_2O} \underset{k_b}{\overset{k_f}{\rightleftharpoons}} \mathrm{MeSCN{\cdot}H_2O + H_3O^+} \quad (2)$$

where k_f is the rate constant for hydronium H-bonded to CN switching to water being H-bonded to CN, and k_b is for the opposite process. From the comparison between eqs 1 and 2, the hydronium to water rate is $k_{HW} \equiv \frac{1}{\tau_{HW}} = k_f[H_2O]$ and the water to hydronium rate is $k_{WH} \equiv \frac{1}{\tau_{WH}} = k_b[H_3O^+]$. For the water concentrations corresponding to the 1:4, 1:5, and 1:6

DOI: 10.1021/acscentsci.9b00447
ACS Cent. Sci. 2019, 5, 1269−1277

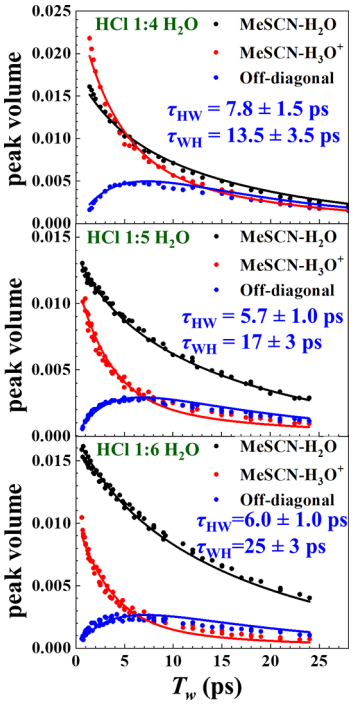

Figure 3. Chemical exchange data (points) for three HCl/water concentrations. τ_{HW} and τ_{WH}: times for the species H-bonded to MeSCN to switch, hydronium to water and water to hydronium, respectively. The solid curves through the data in each panel are fits to the data with one set of fitting parameters giving all three curves. The fits yield the chemical exchange rates.

solutions, k_f = 4.1 ± 0.8, 5.0 ± 0.9, and 4.4 ± 0.7 ns^{-1} M^{-1}, respectively. Within experimental error, k_f is independent of the water concentration over the range studied, with the average k_f = 4.5 ns^{-1} M^{-1}. This independence of k_f on concentration reinforces the validity of the rate scheme.

The exchange rate constants in LiCl solution are about 7 times smaller than those of HCl solution.[32] This large difference resembles the anomalous proton ion mobility compared to Li^+ cations in aqueous solution. There are two mechanisms of proton transport in aqueous solution: vehicular (Stokes) diffusion in which the oxygen atom carrying the extra proton moves through the water and structural diffusion (proton relay) in which the proton hops from one oxygen atom to another with associated hydrogen bond reorganization.[1]

Proton transfer (hopping) is observable as chemical exchange (see Figure 4, left side). There is another mechanism that can also give rise to the observed chemical exchange, replacement (see Figure 4, right side). Replacement can involve movement of the hydronium ion as a whole, but not necessarily. Both proton hopping and replacement convert the N lone pair H-bonded to hydronium (N-hydronium) to an N H-bonded to water (or vice versa) but differ in how this occurs. For proton hopping the N-hydronium is converted to an N-water by transfer of a proton from the hydronium bound to the N lone pair to another water molecule. This leaves the same oxygen H-bonded to the N, and thus the original H-bond is not broken. For replacement, starting with an N-hydronium, a water molecule moves in and forms an H-bond to the N while breaking the one to the hydronium. The hydronium that was bonded to the N is thus physically replaced by a water, but it is still a hydronium. The experimentally observed chemical

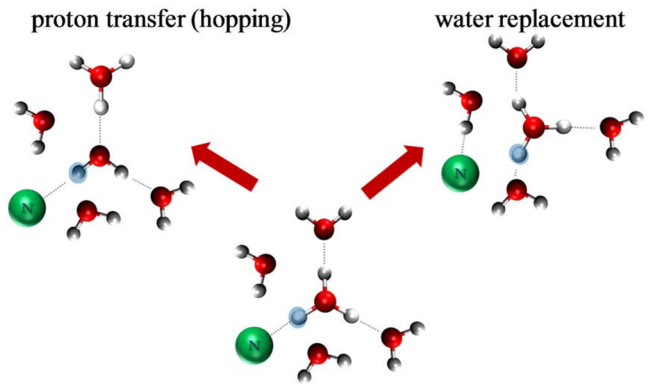

Figure 4. Depiction of the proton transfer and water replacement mechanisms described in the text. Both of these mechanisms result in the N of MeSCN converting from being hydrogen bonded to a hydronium hydrogen (H*) to being hydrogen bonded to water hydrogen (H), but how this occurs differs between them. In the case of proton transfer, the blue shaded H* atom that is initially bound to the N of MeSCN is still hydrogen bonded to N after the transition, but is no longer an H* as it has become an H. A proton has hopped to a different oxygen. In the case of water replacement, the blue shaded H* atom is still an H*, but is no longer hydrogen bonded to the probe. A water has moved in and replaced the hydronium.

exchange cannot distinguish between proton hopping and replacement, but this can be elucidated using AIMD simulations.

B. Simulations. To elucidate the mechanisms observed in the chemical exchange experiments, AIMD simulations were conducted (see Supporting Information). As an initial test of the simulations, orientational relaxation of the probe molecule in neat water was measured and simulated. The experimental and simulated orientational relaxation times of the probe in neat water are 4.7 ± 0.2 ps[32] and 4.8 ps, respectively. In the concentrated HCl solution, the average orientational relaxation time of all probe molecules independent of bonding partner is 5.9 ± 0.4 ps at 10.8 M from experimental and 6.4 ps at 9.8 M from the simulations (see Supporting Information), in excellent agreement. As has been shown previously,[5,33] protons in aqueous solution exist in a wide range of proton-sharing environments between the Eigen and Zundel complexes. Statistically, few protons sit right in the middle between two water molecules as in a standard Zundel complex, and few belong to a strict concept of Eigen complex.[5] However, most protons are closer to one oxygen atom than to another. Therefore, we view the proton defect as a hydronium cation, H_3O^+, and the proton belongs to whichever oxygen it is closest to. A proton hopping event corresponds to a transfer of a proton defect from one oxygen to another, which should be distinguished from the proton rattling events happening on an ~100 fs time scale and leads to the H returning to the same oxygen. In the simulations, we observed fast proton rattling events on the time scale of ~100 fs.

Figure 5A shows the joint probability distribution of the CN stretch frequency and the distance of the closest H atom of a hydronium (H*) to the N (see Supporting Information). Two maxima are observed in this distribution at 1.7 and 3.15 Å, with the former corresponding to H* being H-bonded to the N of the probe and the latter corresponding to a water H-bonded to the N. These maxima correspond to the positions of the first two peaks in the N−H* radial distribution function (RDF) for MeSCN in HCl solution (see Supporting Information). When

DOI: 10.1021/acscentsci.9b00447
ACS Cent. Sci. 2019, 5, 1269−1277

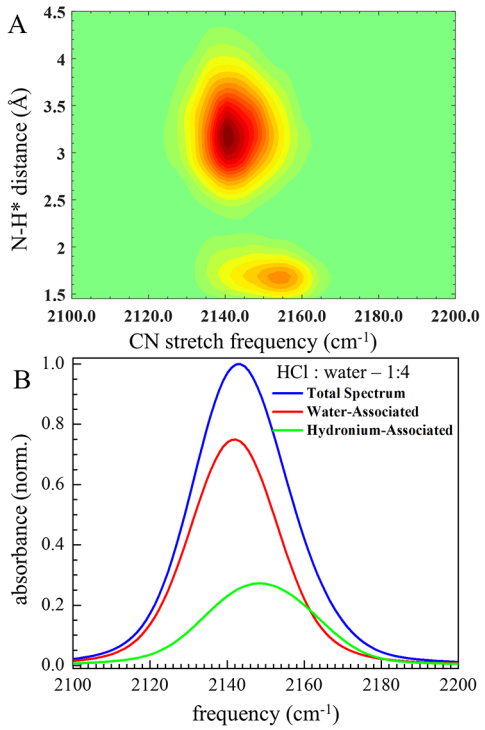

Figure 5. (A) 2D probability distribution of the CN stretch frequency and the distance of the N atom of MeSCN to the closest hydronium hydrogen (H*), obtained from AIMD simulations. (B) Simulated CN stretch spectrum decomposed into water and hydronium bound components.

H* is H-bonded to the N, a higher CN frequency is observed than when it is bound to water. Figure 5B shows the simulated CN stretch vibrational spectrum (blue curve), and the water-bound (red curve) and hydronium-bound (green curve) components. The simulated CN spectrum peak in the acid solution is at 2143 cm^{-1}, which is shifted by −20 cm^{-1} from the experimental spectrum (Figure 1B). Decomposing the peak into the water-bound and hydronium-bound components, using the first minimum in the N−H* RDF to define whether a hydronium is bound or not, gives a splitting between the two species of 7.8 cm^{-1}, compared to the experimental splitting of 7.9 cm^{-1}. To compare the peak intensities obtained from experiment and simulation, the intensity of the hydronium component was multiplied by 1.6 to account for its larger transition dipole determined experimentally (see Supporting Information). Even with this correction included, the hydronium bound peak obtained from the simulation is comparatively lower in intensity than the water one when compared to experiment. This discrepancy is because the simulations predict a slightly lower binding of the hydronium to the probe (20% of the time) than experimentally observed (36% of the time), which corresponds to a ∼0.5 kcal mol^{-1} difference in the free energy between the water and hydronium bound states relative to experiment (see Supporting Information).

To assess the H-bonds formed by the probe, Figure 6 shows the simulated probability distributions of distance vs angle for water and hydronium H-bonding to the MeSCN nitrogen or a water oxygen. For water H-bonding to water or to MeSCN (top panels), the distributions are almost the same. The H-bond of water to N is slightly longer than to oxygen, 1.83 vs 1.78 Å, showing that a MeSCN−water H-bond is only slightly weaker than a water−water H-bond. The angular distributions are almost the same. For hydronium H-bonding to water or MeSCN (bottom panels), the differences are larger; the length of the hydronium−N H-bond is 1.66 Å, while the H-bond to a water oxygen is 1.48 Å, and the hydronium-N H-bond has a broader angular distribution. Therefore, the simulated MeSCN−hydronium H-bond is weaker than the water-hydronium H-bond. The small difference in hydrogen bonding strength causes at most a secondary effect on the observed proton hopping kinetics, as proton hopping occurs between the hydronium and the two water molecules bound to hydronium hydrogens rather than to the nitrogen of the

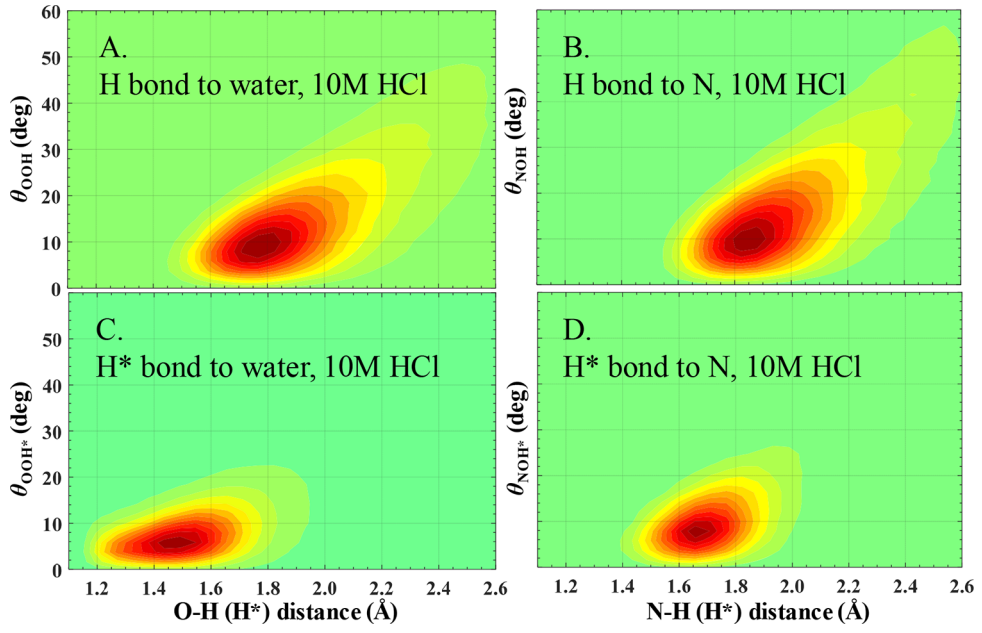

Figure 6. AIMD simulations of distance vs angle, 9.8 M HCl. (A) H of water H-bonded to water. (B) H of water H-bonded to N of MeSCN. (C) H of hydronium H-bonded to water. (D) H of hydronium H-bonded to N of MeSCN.

DOI: 10.1021/acscentsci.9b00447
ACS Cent. Sci. 2019, 5, 1269−1277

MeSCN. In addition, the actual hydrogen bonding difference is smaller than suggested by the simulations because simulations somewhat underestimate the hydronium-bound population as shown by comparison of the experimental and simulated amplitudes of the spectra displayed in Figures 1 and 5, respectively.

In the simulations the off-diagonal peaks grow in with the relaxation to equilibrium with a time constant,

$$\tau_{eq} = 1/(k_{HW} + k_{WH}) \quad (3)$$

For the 10.8 M HCl concentration, the experimental value is τ_{eq} = 4.9 ps, while the simulated value for 9.8 M HCl is 2.2 ps. The faster time constant in the simulations is again consistent with the 0.5 kcal mol^{-1} discrepancy observed in the equilibrium state populations of being bound to water vs hydronium, which, if also applied to the barrier for dissociation, would account for a ~2.3 fold speed-up in the dynamics.

As has been mentioned in the Experiments subsection and illustrated in Figure 4, the dynamics reflected in τ_{eq} can have two contributions, proton hopping and replacement. Our simulations provide a way to assess the relative sizes of these contributions to the rate. In 9.8 M HCl, hopping accounts for 80% of the rate at which a proton defect bound to the MeSCN probe becomes a water bound to the probe (see Supporting Information). Simulations of HCl solutions without the probe present were performed from 0.8 to 10.5 M. In these simulations, with a water replacing the MeSCN as the probe, a hopping component of 90% was obtained at every HCl concentration using the same analysis. The lower hopping percentage when the MeSCN probe is bound to the defect is likely due to the weaker H-bond of hydronium to MeSCN compared to water (Figure 5). The structure and dynamics of concentrated HCl solutions have previously been examined extensively.[34−40] It was suggested that proton structural diffusion may not be the main proton transport mechanism in concentrated HCl due to the low proton conductivity, which could be explained by a regular vehicular mechanism.[40] However, this does not rule out local proton hopping, which our simulation has shown to dominate the chemical exchange kinetics. The low proton conductivity may result from the slowed hydrogen bond rearrangements due to the crowded ionic environment and less extended hydrogen bond network. In pure water, the structural diffusion mechanism is ~5−6 times faster than the vehicular mechanism. As will be shown later, the hydrogen bond rearrangement dynamics, which drive the structural diffusion, are slowed by a factor of around 2 in concentrated HCl solution. Therefore, at high concentration, it is not surprising that the vehicular mechanism provides a larger proportion of the diffusion relative to the structural component.

C. Extrapolation to Infinite Dilution and Determination of the Hopping Time. To determine the proton hopping rate at low acid concentration, several factors must be taken into account. First, the experimental k_f obtained from the probe is concentration independent (4.5 ns^{-1} M^{-1}) within error at the high HCl concentrations studied (10.8, 9.1, and 7.8 M). When extrapolating to the dilute limit using $k_{HW} = k_f[H_2O]$, the change of water concentration is required. Second, at low concentration, a hydronium is H-bonded to three water molecules, giving three pathways for a proton to leave the hydronium. However, with the probe present, at most two of these H* leaving pathways are available since the proton cannot transfer onto the probe itself. In addition, at high concentrations some proton defects are coordinated by Cl^- counterions present in the solution, which also reduces the number of pathways. By performing simulations of aqueous HCl without the probe present from 0.8 to 10.5 M (see Supporting Information), we found that although the total k_f observed varies as a function of acid concentration, the k_f per leaving pathway, or per coordinated water molecule, is *independent* of concentration (see Supporting Information). For example, for acid without the probe present at 0.8, 2, and 10.5 M, the number of leaving paths obtained from our simulations was 3, 2.94, and 2.14, respectively. In the experiments, only proton defects that are bound to MeSCN are observed. Simulations at 9.8 M HCl concentration including the MeSCN probe show that proton defects coordinated to the probe have 1.7 available pathways on average. Overall, the extrapolation from concentrated HCl solution to the dilute limit needs to account for the fraction that is due to hopping (80%), the water concentration increase, and the increase in pathways from 1.7 to 3. Using these factors gives,

$$k_f^{hop} = 0.8 \times (4.5\ ns^{-1}\ M^{-1}) = 3.6\ ns^{-1}\ M^{-1}$$

Using the pure water concentration,

$$k_{HW}^{hop} = k_f^{hop}[H_2O] = k_f^{hop}[55M] = 0.2\ ps^{-1}$$

This value is then increased by 3/1.7 to account for the increase in the number of leaving pathways at low concentration, i.e., k_{HW}^{hop} = 0.35 ps^{-1}, and the hopping time, τ_{hop} = 2.9 ps.

In addition to the three straightforward modifications made above to extrapolate to infinite dilution, there is a physical argument indicating that another correction is in order. Strong experimental support for this argument will be presented below. The water molecules that are H-bonded to the hydronium cation are part of the extended H-bond network. For the proton to hop requires H-bond rearrangement.[5,10,19,21] In pure water, 2D IR spectral diffusion experiments[27,32] (Figure 1A inset) and simulations[27] show that H-bond network rearrangement, which is a concerted process involving many water molecules,[41] is the slowest component of the spectral diffusion. The H-bond network rearrangement in pure water occurs with a time constant of 1.7 ± 0.1 ps (Figure 7).

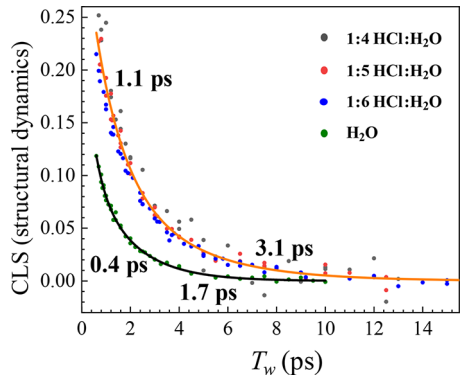

Figure 7. 2D IR data and fits of H-bond structural dynamics in concentrated HCl solutions and pure water showing a factor of ~2 slowing of the H-bond network rearrangement in the HCl solutions (3.1 ps vs 1.7 ps).

DOI: 10.1021/acscentsci.9b00447
ACS Cent. Sci. 2019, 5, 1269−1277

2D IR measurements of the spectral diffusion of the water peak (Figure 1) for all three HCl concentrations and pure water are shown in Figure 7. Because of the overlap of the bands in the HCl solutions, the data are somewhat noisy. The decays for the three data sets are the same within experimental error. The data were fit as one data set. The long time component, 3.1 ± 0.5 ps, indicates that the H-bond network rearrangement is ∼2 faster in pure water than in the HCl solutions. In the dilute limit, a hydronium will be embedded in the extended water H-bond network, which is undergoing rearrangement with a 1.7 ps time constant. Assuming that these water H-bond rearrangements induce the proton hop, it is reasonable that the dilute k_{HW}^{hop} will be a factor of 3.1/1.7 larger than in the HCl solutions, giving $k_{HW}^{hop} \cong 0.64$ ps^{-1}, or the hopping time, τ_{hop} = 1.6 ps.

This value can be compared to τ_{hop} obtained from very low acid concentration conductivity measurements of the proton diffusion constant[23,24] and by NMR.[6] These measurements gave values of τ_{hop} = 1.6−1.8 ps.[6,23,24] The values from mobility and NMR measurements are, within error, the same as the extrapolated value in the dilute limit obtained from the 2D IR chemical exchange experiments.

The chemical exchange measurements of proton hopping extrapolated to infinite dilution gave the same hopping time as determined from proton mobility measurements[23,24] and NMR measurements within error.[6] One of the factors in the extrapolation was the assumption that it was necessary to scale the high HCl concentration hopping time results by the ratio of H-bond rearrangement time in pure water to the time at high HCl concentration as determined by the 2D IR spectral diffusion measurements displayed in Figure 7. This factor with the other factors necessary to go from high acid concentration to the dilute limit gave a hopping time that agreed with the prior more indirect measurements. The agreement suggests that for dilute acid solutions concerted H-bond rearrangement occurring in water is responsible for driving the proton defect to hop from one oxygen to another.

Figure 8 displays the results from temperature-dependent ion mobility measurement determinations of the proton hopping times (red points).[23,29] The black squares are the slowest component of the spectral diffusion (concerted H-bond rearrangement times) measured with 2D IR using the OD stretch of HOD as the vibrational probe in pure H_2O.[30] Within the relatively small experimental error, the temperature-dependent mobility determined hopping times are the same as the pure water H-bond rearrangement times.[30] Therefore, the structural fluctuations that cause the proton to hop are the H-bond rearrangements that occur in the water hydrogen bonded network. In pure water, there are fast local fluctuations of the H-bond network and on a longer time scale, 1.7 ps, the H-bonds of the extended network of water molecules rearrange by the essentially simultaneous switching of the H-bond connectivity among the water molecules (concerted rearrangement). The data in Figure 8 indicate that when a hydronium is part of the extended H-bond water network, it does not have a substantial effect on the switching time, and the process of concerted H-bond rearrangement moves the proton defect from the initial oxygen atom to a different oxygen; i.e., the proton has hopped.

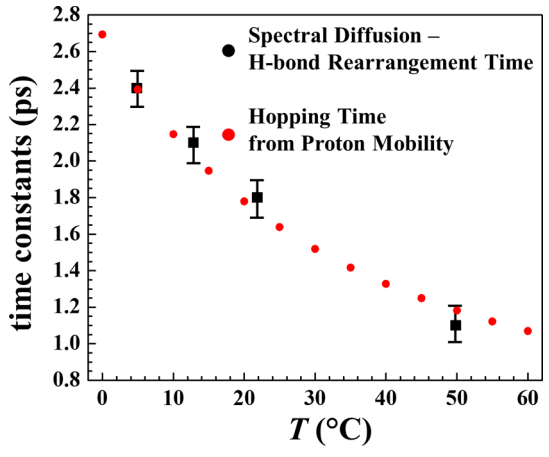

Figure 8. Proton hopping times determined from temperature-dependent ion mobility measurements.[23,29] Slowest component of the spectral diffusion (concerted H-bond rearrangement times) measured with 2D IR using the OD stretch of HOD as the vibrational probe in pure H_2O (black squares).[30]

Safety Statement. No unexpected or unusually high safety hazards were encountered.

III. CONCLUDING REMARKS

We have studied proton hopping in concentrated HCl solutions using 2D IR chemical exchange spectroscopy, spectral diffusion measurements, and ab initio molecular dynamics simulations. To overcome the complexity of the high HCl concentration water spectrum, we employed the CN stretch of MeSCN as the vibrational probe. The CN stretch infrared absorption spectrum can be decomposed into two components, the lower-frequency and higher-frequency sides corresponding to water and hydronium species H-bonded to the nitrogen of the CN, respectively. The 2D IR chemical exchange experiments between the water and hydronium bound states provided the time-dependent kinetics for the hydronium bound species to convert to water and vice versa. This kinetics, as shown by AIMD simulations, is dominated by proton transfer. Therefore, we directly observed the proton hopping, watching a proton defect move from one oxygen atom to another. The experiments gave rates for a hydronium to become a water and for a water to become a hydronium as a function of HCl concentration in concentrated acid solutions. Within experimental error, the rate constants were independent of concentration at high concentration.

The AIMD simulations further showed that the rate constant per proton transfer pathway remains the same from 10 M concentrated HCl solution to low concentration conditions. This enabled extrapolation of the experimental data to the dilute limit. The AIMD simulations provided necessary factors for the extrapolation, i.e., the fraction of chemical exchange events that were caused by proton hopping (80%) rather than replacement (see Figure 4), and the increase in proton defect leaving pathways from 1.7 at high HCl concentration with a bound vibrational probe to 3 in the dilute limit with no probe bound. It was also argued that the H-bond rearrangement necessary for a proton to move between oxygen atoms in the dilute limit has the same time constant as the pure water H-bond rearrangement (see Figure 8). The time constant, which has been determined as the slowest component of the 2D IR spectral diffusion decay, is slower in the concentrated HCl solutions (see Figure 7). Therefore, the hopping rate constant is further increased by the ratio of these time constants (3.1/1.7). With these factors taken into account, the chemical exchange measurements yielded a

DOI: 10.1021/acscentsci.9b00447
ACS Cent. Sci. 2019, 5, 1269−1277

proton hopping time in the dilute limit of 1.6 ps. This time constant is the same as previously reported determinations using NMR line shape[6] and proton mobility measurements (1.6−1.8 ps).[23,24,29]

The proposition that in the dilute limit the proton defect moves from one oxygen atom to another with a time constant determined by concerted hydrogen bond rearrangement with the time constant (1.7 ps) that occurs in pure water was confirmed by experiments. Comparing the temperature dependence of the proton hopping time from mobility measurements to the concerted H-bond rearrangement time in pure water determined by 2D IR measurements showed that they are identical.[23,29,30]

In summary, direct measurements of proton hopping with 2D IR chemical exchange experiments and AIMD simulations yields the proton hopping time in highly concentrated HCl solutions. These results were extrapolated to the dilute limit, and the results explicated the driving mechanism for proton hopping.

■ ASSOCIATED CONTENT

Supporting Information

The Supporting Information is available free of charge on the ACS Publications website at DOI: 10.1021/acscentsci.9b00447.

Supplementary Text Figures S1−S12 and Tables S1−S3 (PDF)

■ AUTHOR INFORMATION

Corresponding Authors

*(T.E.M.) E-mail: tmarkland@stanford.edu.
*(M.D.F.) E-mail: fayer@stanford.edu.

ORCID

Rongfeng Yuan: 0000-0002-6572-2472
Ondrej Marsalek: 0000-0002-8624-8837
Thomas E. Markland: 0000-0002-2747-0518
Michael D. Fayer: 0000-0002-0021-1815

Present Address

§(C.Y.) Department of Chemistry, University of California, Berkeley, California 94720, United States

Author Contributions

#R.Y. and J.A.N. made an equal contribution.

Funding

T.E.M. was supported by the Department of Energy, Office of Basic Energy Sciences CTC and CPIMS programs, under Award Number DE-SC0014437 and the Camille Dreyfus Teacher-Scholar Awards Program. In addition, this work was supported by the Division of Chemical Sciences, Geosciences, and Biosciences, Office of Basic Energy Sciences of the U.S. Department of Energy through Grant No. DEFG03-84ER13251 (R.Y., M.D.F.), and in part by the Air Force Office of Scientific Research under AFOSR Award No. FA9550-16-1-0104 (C.Y., M.D.F., and the 2D IR spectrometer). O.M. was supported by the grant Primus 16/SCI/27/247019. This research used resources of the National Energy Research Scientific Computing Center, a DOE Office of Science User Facility supported by the Office of Science of the U.S. Department of Energy under Contract No. DE-AC02-05CH11231.

Notes

The authors declare no competing financial interest.

■ ACKNOWLEDGMENTS

We would like to thank Professors John I. Brauman and Hans C. Andersen, Stanford University, for their helpful input.

■ REFERENCES

(1) Marx, D. Proton transfer 200 years after von Grotthuss: Insights from ab initio simulations. *ChemPhysChem* **2006**, *7*, 1848−1870.
(2) de Grotthuss, C. On the decomposition of water and of the bodies that it holds in solution by means of galvanic electricity. *Ann. Chim.* **1806**, *58*, 54−73.
(3) Hynes, J. T. The protean proton in water. *Nature* **1999**, *397*, 565−567.
(4) Day, T. J. F.; Schmitt, U. W.; Voth, G. A. The mechanism of hydrated proton transport in water. *J. Am. Chem. Soc.* **2000**, *122*, 12027−12028.
(5) Napoli, J. A.; Marsalek, O.; Markland, T. E. Decoding the spectroscopic features and time scales of aqueous proton defects. *J. Chem. Phys.* **2018**, *148*, 222833.
(6) Meiboom, S. Nuclear magnetic resonance study of proton transfer in water. *J. Chem. Phys.* **1961**, *34*, 375.
(7) Woutersen, S.; Bakker, H. J. Ultrafast vibrational and structural dynamics of the proton in liquid water. *Phys. Rev. Lett.* **2006**, *96*, 138305.
(8) Marx, D.; Tuckerman, M. E.; Hutter, J.; Parrinello, M. The nature of the hydrated excess proton in water. *Nature* **1999**, *397*, 601−604.
(9) Markovitch, O.; Chen, H.; Izvekov, S.; Paesani, F.; Voth, G. A.; Agmon, N. Special pair dance and partner selection: Elementary steps in proton transport in liquid water. *J. Phys. Chem. B* **2008**, *112*, 9456−9466.
(10) Hassanali, A.; Giberti, F.; Cuny, J.; Kuhne, T. D.; Parrinello, M. Proton transfer through the water gossamer. *Proc. Natl. Acad. Sci. U. S. A.* **2013**, *110*, 13723−13728.
(11) Geissler, P. L.; Dellago, C.; Chandler, D.; Hutter, J.; Parrinello, M. Autoionization in liquid water. *Science* **2001**, *291*, 2121−2124.
(12) Dahms, F.; Fingerhut, B. P.; Nibbering, E. T. J.; Pines, E.; Elsaesser, T. Large-amplitude transfer motion of hydrated excess protons mapped by ultrafast 2D IR spectroscopy. *Science* **2017**, *357*, 491−494.
(13) Dahms, F.; Costard, R.; Pines, E.; Fingerhut, B. P.; Nibbering, E. T. J.; Elsaesser, T. The Hydrated Excess Proton in the Zundel Cation $H_5O_2^+$: The Role of Ultrafast Solvent Fluctuations. *Angew. Chem., Int. Ed.* **2016**, *55*, 10600−10605.
(14) Kulig, W.; Agmon, N. A 'clusters-in-liquid' method for calculating infrared spectra identifies the proton-transfer mode in acidic aqueous solutions. *Nat. Chem.* **2013**, *5*, 29−35.
(15) Fournier, J. A.; Carpenter, W. B.; Lewis, N. H. C.; Tokmakoff, A. Broadband 2D IR spectroscopy reveals dominant asymmetric $H_5O_2^+$ proton hydration structures in acid solutions. *Nat. Chem.* **2018**, *10*, 932−937.
(16) Carpenter, W. B.; Fournier, J. A.; Lewis, N. H. C.; Tokmakoff, A. Picosecond proton transfer kinetics in water revealed with ultrafast IR spectroscopy. *J. Phys. Chem. B* **2018**, *122*, 2792−2802.
(17) Thamer, M.; De Marco, L.; Ramasesha, K.; Mandal, A.; Tokmakoff, A. Ultrafast 2D IR spectroscopy of the excess proton in liquid water. *Science* **2015**, *350*, 78−82.
(18) Wolke, C. T.; Fournier, J. A.; Dzugan, L. C.; Fagiani, M. R.; Odbadrakh, T. T.; Knorke, H.; Jordan, K. D.; McCoy, A. B.; Asmis, K. R.; Johnson, M. A. Spectroscopic snapshots of the proton-transfer mechanism in water. *Science* **2016**, *354*, 1131−1135.
(19) Biswas, R.; Tse, Y. L.; Tokmakoff, A.; Voth, G. A. Role of Presolvation and Anharmonicity in Aqueous Phase Hydrated Proton Solvation and Transport. *J. Phys. Chem. B* **2016**, *120*, 1793−1804.
(20) Meng, X. Z.; Guo, J.; Peng, J. B.; Chen, J.; Wang, Z. C.; Shi, J. R.; Li, X. Z.; Wang, E. G.; Jiang, Y. Direct visualization of concerted proton tunnelling in a water nanocluster. *Nat. Phys.* **2015**, *11*, 235−239.

DOI: 10.1021/acscentsci.9b00447
ACS Cent. Sci. 2019, 5, 1269−1277

(21) Tse, Y. L. S.; Knight, C.; Voth, G. A. An analysis of hydrated proton diffusion in ab initio molecular dynamics. *J. Chem. Phys.* **2015**, *142*, 014104.
(22) Headrick, J. M.; Diken, E. G.; Walters, R. S.; Hammer, N. I.; Christie, R. A.; Cui, J.; Myshakin, E. M.; Duncan, M. A.; Johnson, M. A.; Jordan, K. D. Spectral signatures of hydrated proton vibrations in water clusters. *Science* **2005**, *308*, 1765−1769.
(23) Light, T. S.; Licht, S.; Bevilacqua, A. C.; Morash, K. R. The fundamental conductivity and resistivity of water. *Electrochem. Solid-State Lett.* **2005**, *8*, E16−E19.
(24) Agmon, N. The Grotthuss Mechanism. *Chem. Phys. Lett.* **1995**, *244*, 456−462.
(25) Carpenter, W. B.; Fournier, J. A.; Biswas, R.; Voth, G. A.; Tokmakoff, A. Delocalization and stretch-bend mixing of the HOH bend in liquid water. *J. Chem. Phys.* **2017**, *147*, 084503.
(26) Eigen, M. Proton Transfer Acid-Base Catalysis + Enzymatic Hydrolysis. I. Elementary Processes. *Angew. Chem., Int. Ed. Engl.* **1964**, *3*, 1−19.
(27) Asbury, J. B.; Steinel, T.; Stromberg, C.; Corcelli, S. A.; Lawrence, C. P.; Skinner, J. L.; Fayer, M. D. Water Dynamics: Vibrational Echo Correlation Spectroscopy and Comparison to Molecular Dynamics Simulations. *J. Phys. Chem. A* **2004**, *108*, 1107−1119.
(28) Moilanen, D. E.; Wong, D.; Rosenfeld, D. E.; Fenn, E. E.; Fayer, M. D. Ion-water hydrogen-bond switching observed with 2D IR vibrational echo chemical exchange spectroscopy. *Proc. Natl. Acad. Sci. U. S. A.* **2009**, *106*, 375−380.
(29) Mills, R. A Remeasurement of the Self-Diffusion Coefficients of Sodium Ion in Aqueous Sodium Chloride Solutions. *J. Am. Chem. Soc.* **1955**, *77*, 6116−6119.
(30) Nicodemus, R. A.; Corcelli, S. A.; Skinner, J. L.; Tokmakoff, A. Collective Hydrogen Bond Reorganization in Water Studied with Temperature-Dependent Ultrafast Infrared Spectroscopy. *J. Phys. Chem. B* **2011**, *115*, 5604−5616.
(31) Zheng, J.; Kwak, K.; Asbury, J. B.; Chen, X.; Piletic, I. R.; Fayer, M. D. Ultrafast Dynamics of Solute-Solvent Complexation Observed at Thermal Equilibrium in Real Time. *Science* **2005**, *309*, 1338−1343.
(32) Yuan, R.; Yan, C.; Fayer, M. Ion−molecule complex dissociation and formation dynamics in LiCl aqueous solutions from 2D IR spectroscopy. *J. Phys. Chem. B* **2018**, *122*, 10582−10592.
(33) Daly, C. A.; Streacker, L. M.; Sun, Y. C.; Pattenaude, S. R.; Hassanali, A. A.; Petersen, P. B.; Corcelli, S. A.; Ben-Amotz, D. Decomposition of the Experimental Raman and Infrared Spectra of Acidic Water into Proton, Special Pair, and Counterion Contributions. *J. Phys. Chem. Lett.* **2017**, *8*, 5246−5252.
(34) Agmon, N. Structure of Concentrated HCl Solutions. *J. Phys. Chem. A* **1998**, *102*, 192−199.
(35) Botti, A.; Bruni, F.; Imberti, S.; Ricci, M. A.; Soper, A. K. Ions in water: the microscopic structure of a concentrated HCl solution. *J. Chem. Phys.* **2004**, *121*, 7840−7848.
(36) Stoyanov, E. S.; Stoyanova, I. V.; Reed, C. A. The structure of the hydrogen ion (H_{aq}^{+}) in water. *J. Am. Chem. Soc.* **2010**, *132*, 1484−1485.
(37) Baer, M. D.; Fulton, J. L.; Balasubramanian, M.; Schenter, G. K.; Mundy, C. J. Persistent ion pairing in aqueous hydrochloric acid. *J. Phys. Chem. B* **2014**, *118*, 7211−7220.
(38) Xu, J.; Izvekov, S.; Voth, G. A. Structure and dynamics of concentrated hydrochloric acid solutions. *J. Phys. Chem. B* **2010**, *114*, 9555−9562.
(39) Mancinelli, R.; Sodo, A.; Bruni, F.; Ricci, M. A.; Soper, A. K. Influence of concentration and anion size on hydration of H^{+} ions and water structure. *J. Phys. Chem. B* **2009**, *113*, 4075−4081.
(40) Dippel, T.; Kreuer, K. D. Proton transport mechanism in concentrated aqueous solutions and solid hydrates of acids. *Solid State Ionics* **1991**, *46*, 3−9.
(41) Laage, D.; Hynes, J. T. A Molecular Jump Mechanism of Water Reorientation. *Science* **2006**, *311*, 832−835.

DOI: 10.1021/acscentsci.9b00447
ACS Cent. Sci. 2019, 5, 1269−1277